A pragmatic approach for engineering porous mannitol and mechanistic evaluation of particle performance

Ali Al-Khattawi[1], Jasdip Koner[1,2], Peter Rue[1], Dan Kirby[1,2], Yvonne Perrie[1,2,] Ali Rajabi-Siahboomi[3], Afzal R Mohammed[1,2]*

[1] Aston Pharmacy School, Aston University, Birmingham, B4 7ET, UK

[2] Aston Research Centre for Children and Young People's Health (ARCHY), Aston University, Birmingham, B4 7ET.

[3] Colorcon, Inc., Harleysville, PA 19438, USA.

*** Corresponding Author:**

Afzal R Mohammed

Aston Pharmacy School, Aston University, Birmingham, B4 7ET, UK

Email: a.u.r.mohammed@aston.ac.uk

Phone: +44(0) 121-204 4183

Abstract

The importance of mannitol has increased recently as an emerging diluent for orodispersible dosage forms. The study aims to prepare spray dried mannitol retaining high porosity and mechanical strength for the development of orally disintegrating tablets (ODTs).

Aqueous feed of D-mannitol (10% w/v) comprising ammonium bicarbonate, NH_4HCO_3 (5% w/v) as pore former was spray dried at inlet temperature of 110-170°C. Compacts were prepared at 20 kN and characterized for porosity, hardness and disintegration time. Particle morphology and drying mechanisms were studied using thermal (HSM, DSC and TGA) and polymorphic (XRD) methods.

Tablet porosity increased from 0.20 ± 0.002 for pure mannitol to 0.53 ± 0.03 using fabricated porous mannitol. Disintegration time dropped by 50-77% from 135 ± 5.29 sec for pure mannitol to 75.33 ± 2.52 - 31.67 ± 1.53 sec for mannitol 110 - 170°C. Hardness increased by 150% at 110°C (258.67 ± 28.89 N) and 30% at 150°C (152.70 ± 10.58 N) compared to pure mannitol tablets (104.17 ± 1.70 N). Increasing inlet temperature resulted in reducing tablet hardness due to generation of 'micro-sponge'-like particles exhibiting significant elastic recovery. Impact of mannitol polymorphism on plasticity/elasticity cannot be ruled out as a mixture of α and β polymorphs formed upon spray drying.

Keywords: Mannitol, porosity, orally disintegrating tablet, spray drying, plasticity, hardness, particle engineering.

Introduction

Mannitol is a versatile excipient with physical state that may be engineered to meet the diverse needs of formulation development of special dosage forms [1]. The last decade has seen the commercial introduction of a number of mannitol products with properties tailored to orally disintegrating dosage forms [2]. Popularity of mannitol was attributed to many factors including low hygroscopicity, inertness to APIs and development of robust tablets [3].

Most non-processed mannitol products suffer poor mechanical properties due to brittle fracture under pressure [4 - 5]. The development of orally disintegrating tablets (ODTs) requires more than just good binding properties in an excipient [2]. An ideal ODT excipient would provide favourable disintegration profile (around 30 sec) in addition to high mechanical strength. The fast disintegration property is usually attained by reducing the compression force during tableting thereby increasing inter-particle voids; however, this approach leads to weak and fragile tablets [6].

Particle engineering via spray drying may constitute a way for improving internal porosity and physico-mechanical properties of mannitol based ODT by controlling particle characteristics using subliming pore formers [7]. Previous research has shown that ammonium bicarbonate (NH_4HCO_3) sublimes above 50°C and removed directly during spray drying [8]. This property of NH_4HCO_3 as a pore former was also termed the 'baking powder effect' whereby the material leaves voids in formulated particles due to evolution of $H_2O\uparrow$, $NH_3\uparrow$ and $CO_2\uparrow$ [9]. Koizumi et al. [10] attempted the inclusion of volatile additive Camphor in an ODT base followed by batch vacuum/heating process to sublime the material. Despite this, the crushing strength of the produced tablets was insufficient as the increase in porosity was concomitant with a decrease in the structural integrity of tablet.

On the other hand, spray drying potentially provides a continuous and cost-effective platform for the production of mannitol with enhanced porosity [11]. Another added advantage is the tablet mechanical

strength improvement after spray drying which is thought to be linked to more compressible amorphous material generation or better die rearrangement of particles [12 - 13].

Understanding the morphological and physico-chemical and mechanical properties of mannitol during processing is also important as the excipient shows multiple polymorphic phases, e.g. α, β, δ [14 - 16]. In fact, spray drying of mannitol may produce one or more polymorphic forms with varying morphologies depending on the temperature of drying or the use of adjuvant excipients [1], [17], [18] .

The primary hypothesis in this article is built on material processing of mannitol to overcome the significant challenges of low porosity and weak mechanical strength of mannitol based ODT. This may be achieved through the fabrication of spherical, porous and resilient particles using spray drying. The objective of the work in the current study was to fabricate compressible particles of mannitol that would resist the application of high compression forces during tableting overcoming particle fracture together with exploiting the porous anatomy of the resultant particles to promote tablet disintegration through 'wicking'.

Materials and methods

Materials

D-mannitol (≥98.0% pure) and ammonium bicarbonate (NH_4HCO_3, ≥99.0% pure) were purchased from Sigma-Aldrich (Pool, UK). Both materials were in powder form and used as received.

Methods

Preparation of spray dried porous mannitol particles

Particles of mannitol were fabricated by spray drying an aqueous feed solution composed of D-mannitol and ammonium bicarbonate dissolved in distilled water. Preliminary experiments involved using 10-70% w/v D-mannitol and 5 - 20% w/v ammonium bicarbonate. Optimized formula for which most of the characterization was carried out was made using 2:1 ratio, 10% w/v mannitol: 5% w/v ammonium bicarbonate. Laboratory-scale Mini Spray Dryer B-290 from Buchi (Flawil, Switzerland) equipped with

1.5 mm nozzle was used for the procedure. The spray drying conditions were: co-current air flow rate of 670 NormLitre/h, 90% aspirator rate, 145 mL/h pump rate and inlet temperature of 110 - 170°C. A control formulation was also prepared containing 10% w/v mannitol without ammonium bicarbonate for particle morphology comparison. Process yield (%) was calculated after each run using Eq. (1):

$$\text{Yield}\ (\%) = \frac{\text{Mass of solids after spray drying}}{\text{Mass of solids before spray drying}} \times 100 \text{.....Eq. (1)}$$

Powder flow assessment by bulk and tapped density measurements

Bulk and tapped densities were measured using a Sotax tap density tester USP II apparatus (Allschwil, Switzerland). The test parameters followed the official USP monograph <616> [19] except for cylinder volume which was smaller (5 mL) and weight of sample (2 g) due to limited powder quantities. Hausner ratio and Carr's index were calculated for the samples using Eq. (2) and Eq. (3):

$$\text{Hausner ratio} = \frac{\text{Tapped density}}{\text{Bulk density}} \text{.....Eq. (2)}$$

$$\text{Carr's Index} = \frac{(\text{Tapped density} - \text{Bulk density})}{\text{Tapped density}} \times 100 \text{.....Eq. (3)}$$

Particle size analysis

Particle Size measurements were carried out using Sympatec (Clausthal-Zellerfeld, Germany) laser diffraction particle size analyzer according to the experimental procedure detailed in [20]. Volume mean diameter (VMD) was recorded.

Tablet preparation

A bench-top hydraulic press from Specac ltd. (Slough, UK) was used to compress pure and fabricated mannitol powders into 500 mg, 13 mm flat-faced tablets. Magnesium stearate (0.5% w/w) was added to each formulation followed by compression at 20 kN.

Helium pycnometry for true density and porosity measurement

True density and porosity were measured for all the powders/tablets using a helium multipycnometer from Quantachrome Instruments (Syosset, USA). Each powder (1000 mg) or tablet (500 mg) was placed into a micro sample cell and assessed for true volume and in turn true density. Detailed methodology is

reported elsewhere [20]. Bulk density measurement for tablet was carried out and porosity (ε) calculated using Eq. (4):

$$\varepsilon = 1 - \frac{\text{bulk density}}{\text{true density}} \text{.....Eq. (4)}$$

Tablet hardness and disintegration time

Hardness (diametral crushing strength) of tablets was measured using 4M tablet hardness tester from Schleuniger (Thun, Switzerland). Disintegration time was determined using the USP moving basket apparatus [21] from Erweka (Erweka ZT3, Heusenstamm, Germany). Measurements were performed individually to improve accuracy of recording.

Heckel profile analysis

In-die Heckel plots were obtained by compressing the powders of pure (unmodified) and fabricated mannitol between 0 - 40 MPa using a Hounsfield materials testing machine from Tinius Olsen (Pennsylvania, USA). The machine was equipped with 13 mm diameter flat-faced punches. Die and punches were externally lubricated with magnesium stearate dispersed in acetone (5% w/v) prior to each measurement. Each powder (500 mg) was manually filled into the die before starting the compression cycle. The lower punch was stationary during the compression while the upper punch moved at a speed of 6.66 mm/sec. Corrections for tablet thickness and weight were made after each compression cycle to account for punch elastic compressive strains and displacement errors. From the Heckel plot i.e. ln(1/(1-D)) vs. compaction pressure, the slope (K) and intercept (A) of the terminal linear region (above 30 MPa) with the best R^2 value was obtained. Reciprocal of K is the apparent yield pressure (Py) of material.

Compressive stress/strain curves

Tablets of pure and fabricated mannitol (500 mg, 13 mm diameter) were prepared at 12-30 kN and tested for compressive stress/strain profile using texture analyzer from Brookfield (Massachusetts, USA). The instrument was equipped with 50 kg load cell, TA44 probe (4 mm diameter, cylindrical) and TA-BT KIT table fixture. Test target was 5% deformation in the axial direction without breaking the tablet. Both tablet height and diameter were measured manually before the test (using a digital caliper) and information fed

into the instrument software. The test was carried out on the centre of the specimen at a trigger load of 50 g and a probe speed of 3 mm/sec. The stress/strain curves for consecutive loading and unloading cycles were recorded and area in between calculated using GraphPad Prism 6.02 software (California, USA).

Scanning electron microscopy (SEM)

The morphology of mannitol powders and tablets' cross-sections was examined using scanning electron microscope XL30 FEG ESEM from Philips (Amsterdam, Netherlands). For the powders, approximately 1 mg of each material was sprinkled onto a double-sided adhesive strip on an aluminium stub. For the tablets, each of the 500 mg compacts was dissected with a blade then a thin section was obtained to improve gold coating of the specimen. The specimen stub was coated with a thin layer of gold using a sputter coater Polaron SC500 from Polaron Equipment ltd. (Watford, UK) at 20 mA for 3 min followed by sample examination using SEM. The acceleration voltage (kV) and the magnification were recorded on each micrograph.

Differential scanning calorimetry (DSC)

DSC Q200, from TA Instruments (Delaware, USA) was used to determine the thermal properties of powders. Temperature heat flow was calibrated with Indium (Melting point 156.8°C). Accurately weighed samples (3 mg each) of pure and fabricated mannitol were transferred into non-hermetically sealed Tzero pans. Each sample was heated at 10°C/min from 30 - 200°C under a nitrogen purge (50 mL/min). This was followed by analysis of resulting thermograms using TA instruments universal analysis 2000 software (V 4.5A).

Thermogravimetric analysis (TGA)

A thermogravimetric analyzer Pyris 1 TGA from Perkin Elmer (Massachusetts, USA) was used to measure the moisture content (%) and decomposition temperature of pure mannitol, fabricated mannitol and ammonium bicarbonate. Each sample (2 mg) was loaded onto the TGA pan and heated at 10°C/min from 30 - 300°C under nitrogen stream (20 mL/min). Pyris Manager Software (version 5.00.02) was used for analysing the obtained thermograms. Moisture content was calculated between 70 and 120°C.

Hot stage microscopy (HSM)

To monitor the drying kinetics and particle formation, HSM was carried out according to the method reported in [18] using a Nikon Eclipse LV100 polarizing microscope from Nikon Instruments (Amsterdam, Netherlands) equipped with a Linkam hot stage (Surrey, UK). A droplet (4 mm diameter) of mannitol (10% w/v) and ammonium bicarbonate (5% w/v) formulation was placed on a microscope slide pre-heated to the spray drying temperatures 110, 150 and 170°C. Photomicrographs were captured for the crystallization/drying of droplets at the different temperatures using 1.3 Mega Pixel Moticam camera and software from Motic (Hong Kong, China).

X-ray diffraction (XRD)

D2 Phaser X-ray diffractometer from Bruker (Massachusetts, USA) was used for analyzing the polymorphic types of mannitol powders and tablets. The angular range (2θ) was 4 – 50° with increments steps of 0.02° and measured at 0.25 sec/step. Diffractive patterns were generated as counts per step and thereafter analyzed using Eva 18.0.0.0 software (Bruker, AXS). Material Analysis Using Diffraction (MAUD) software 2.49 (Luca Luterotti, University of California, USA) was used to quantify the polymorphic content of the mannitol powders through Rietveld Refinement. Calculated patterns for the mannitol polymorphs were obtained from the Cambridge Crystallographic Data Centre and imported into MAUD as .cif files, obtained XRD patterns were then fitted to the calculated patterns and percentages of each polymorph calculated.

Statistical analysis

ANOVA followed by Tukey post-hoc test and student t-test were performed using GraphPad Prism 6.02 software (California, USA). Statistical significant difference was considered at a p value <0.05. Where applicable, all results are presented as mean ± standard deviation for triplicate measurements to account for the noise encountered within the experiments. For DSC, TGA and XRD, representative thermograms/diffraction patterns were presented out of the triplicate measurements.

Results and discussion

Morphology, porosity and micromeritic properties

Morphological studies using SEM generally showed spherical particles for fabricated mannitol in comparison with pure mannitol which had a columnar or prismatic rod-shaped particle (Figure 1 c, e, g and a). In addition, the formed particles appear to have surface gaps/pores unlike pure mannitol particles. Mannitol made at 110°C (outlet temp. 60°C, shown in c) has irregular shape possibly due to incomplete particle formation whereas those made at higher temperatures 150°C (outlet temp. 80°C, shown in e) and 170°C (outlet temp. 90°C, shown in g) resulted in spherical particles. Surface pores are evident for particles sprayed at 150°C and less visible for particle made at 170°C. The role of ammonium bicarbonate in creating surface pores was confirmed by comparing fabricated mannitol morphology to a control formulation (containing no NH_4HCO_3) (shown in b). The latter clearly showed a smooth surface with no surface gaps at all.

Initial investigations were carried out to observe the effect of NH_4HCO_3 on porosity. Helium pycnometry measurements showed 14% higher porosity (0.91 ± 0.03) for the powder made from 10% w/v mannitol and 10% w/v NH_4HCO_3 than pure mannitol powder (0.77 ± 0.02). By tableting at 20 kN, the porosity of spray dried mannitol reduced to 0.45 ± 0.03, however, it was still significantly higher (t-test, $p<0.001$) than porosity of tablets made from pure mannitol (0.20 ± 0.002). Furthermore, the reduction of NH_4HCO_3 to 5% w/v (mannitol also at 10% w/v) resulted in further increase of tablet porosity (0.53 ± 0.03) compared to 10% w/v NH_4HCO_3 (0.45 ± 0.03). In fact, an overall 33% enhancement in tablet porosity was achieved with spray dried mannitol (using 5% w/v of NH_4HCO_3) compared to pure mannitol.

The increase in porosity upon reduction of ammonium bicarbonate contradicted the hypothesis that pore former quantity is directly related to porosity. It could be that an optimum amount of ammonium bicarbonate was required to achieve maximum porosity whereby any further increase in the pore former would not cause significant improvement. This may also be related to the nature of spray drying process whereby heat-mass transfer and particle crust formation is best achieved using an optimal concentration

of solids in the feed solution [22 - 23]. In fact, this was confirmed as attempts to use higher amounts of ammonium bicarbonate (up to 20% w/v) and mannitol (up to 70% w/v) did not result in further enhancement of porosity. This was possibly due to increased solid content (i.e. higher density) in formed particles upon increase in spray drying feed concentration.

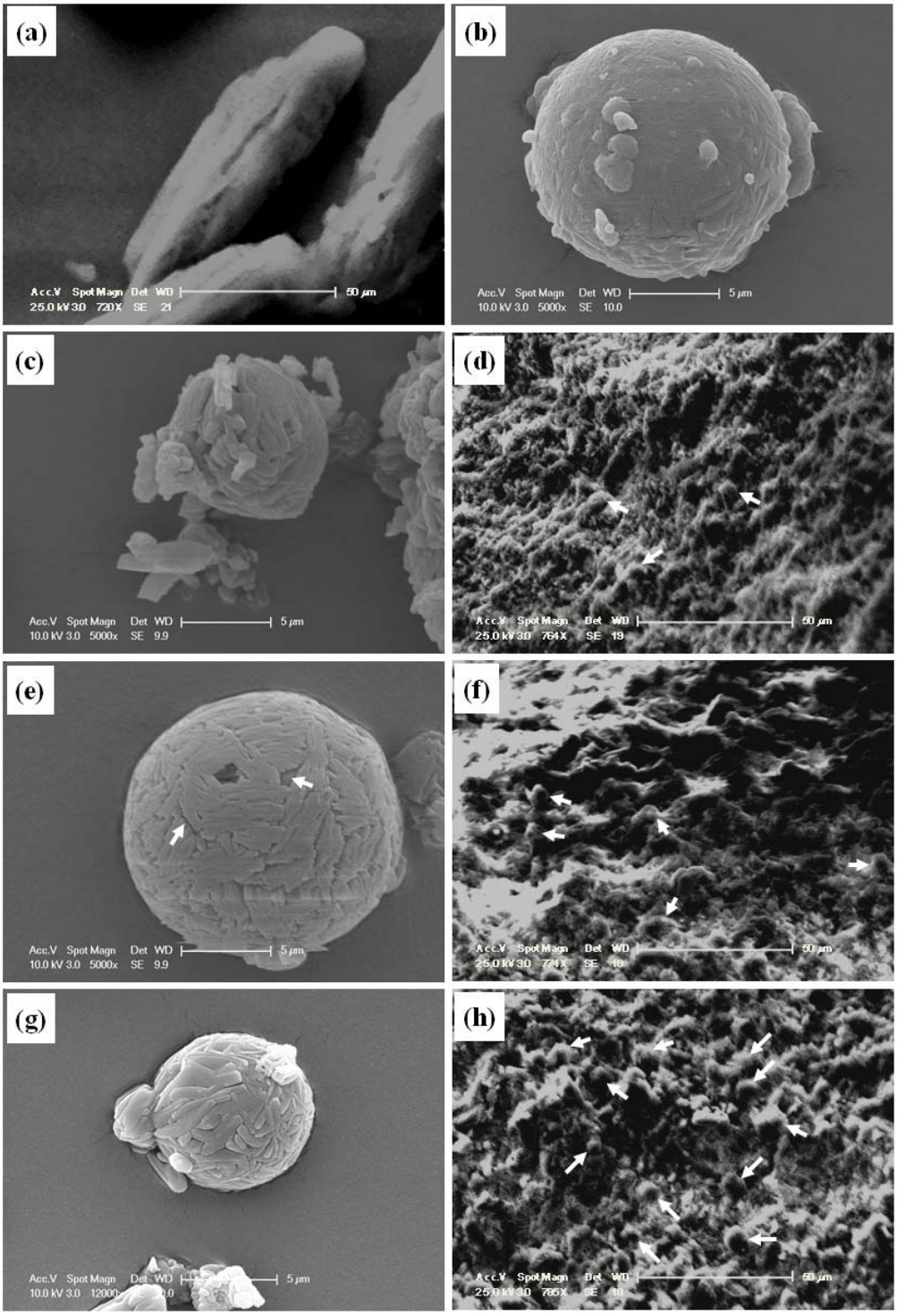

Figure 1: SEM showing morphology of mannitol particles and tablets (at 20 kN), (a) pure mannitol powder as control, (b) mannitol spray dried without NH_4HCO_3 as 2nd control, (c) and (d) mannitol sprayed with NH_4HCO_3 at 110°C and compact, (e) and (f) mannitol sprayed with NH_4HCO_3 at 150°C (arrows on gaps) and compact, (g) and (h) mannitol sprayed with NH_4HCO_3 at 170°C and compact, (Arrows in (d),(f),(h) point to spherical particles after tableting).

Porosity and other micromeritic properties of the powders produced at 110 - 170°C are summarized in Table 1. Porosity after tableting was preferred over powders' porosity due to difficulty to accurately measure powder dimensions and bulk volume (Table 1). Tablets made from mannitol fabricated at 110 - 170°C showed significantly (ANOVA, $p<0.001$) higher porosity (0.30 ± 0.001 - 0.53 ± 0.03) when compared to pure mannitol tablets (0.20 ± 0.002). This was consistent with the significantly lower (ANOVA, $p<0.001$) true density of spray dried mannitol (1.50 ± 0.003 - 1.54 ± 0.004 g/cm^3) than pure mannitol (1.60 ± 0.002 g/cm^3). The powder made at 170°C showed significantly higher porosity (ANOVA/Tukey, $p<0.05$) than the rest of the powders which was attributed to particles elasticity and resistance to crushing (see discussion on elasticity measurements under physico-mechanical properties).

Analysis of particle size measurements for the processed mannitol when compared to non-processed mannitol showed a significant drop in size (ANOVA, $p<0.001$). Similarly, Carr's index showed an extremely poor flowability (> 40%) while Hausner ratio indicated the powder requires special agitation or hopper (> 1.6). However, these properties are not too dissimilar to the pure mannitol which was on the borderline for extremely poor flow (39.5 ± 1.56) of the Carr's index and has a Hausner ratio above 1.6 indicating requirement of assisted flow.

Table 1: Porosity and micromeritic properties of pure and fabricated mannitol (10% w/v mannitol and 5% w/v ammonium bicarbonate) spray dried at 110 - 170°C. Results reported as mean ± SD (n=3).

Mannitol	Porosity after tableting	Powder True density (g/cm^3)	Particle size (VMD)	Carr's index (%)	Hausner's ratio	Moisture content (%)	Yield (%)
Pure	0.20 ± 0.002	1.60 ± 0.002	35.41 ± 1.85	39.5 ± 1.56	1.65 ± 0.04	0.12 ± 0.10	-
Sprayed at 110°C	0.30 ± 0.001	1.50 ± 0.003	17.93 ± 1.29	56 ± 1.49	2.27 ± 0.08	0.51 ± 0.43	7.55 ± 4.77
Sprayed at 150°C	0.28 ± 0.01	1.49 ± 0.005	16.03 ± 0.48	68.79 ± 0.14	3.2 ± 0.01	0.23 ± 0.11	41.83 ± 9.03
Sprayed at 170°C	0.53 ± 0.03	1.54 ± 0.004	13.32 ± 0.93	64.77 ± 8.88	2.95 ± 0.67	0.19 ± 0.11	22.77 ± 0.67

Investigation of the moisture content using TGA yielded < 1% moisture content for all the different spray dried powders. Moisture content was inversely proportional to increase in inlet temperature. The yield of the process was lowest at 110°C due to insufficient drying and sticking to drying chamber and highest at 150°C followed by a lower yield again at 170°C (Table 1). The latter was attributed to deposition on instrument walls due to proximity to mannitol's melting point (165°C) which renders the material sticky.

Physico-mechanical properties

Results showed that spraying a formulation containing 10% w/v mannitol and 5% w/v ammonium bicarbonate not only provides relatively high porosity (as mentioned above), but also high mechanical strength to the resultant tablets. Spraying the formulation at inlet temperature of 110 - 170°C provided tablet hardness of 258.67 ± 28.89 - 98.53 ± 15.24 N (Table 2). This constitutes a 150% increase (ANOVA/Tukey, $p<0.001$) in hardness for mannitol sprayed at 110°C (258.67 ± 28.89 N) and 30% increase (ANOVA/Tukey, $p<0.05$) for mannitol sprayed at 150°C (152.70 ± 10.58 N) compared to pure mannitol (104.17 ± 1.70 N). However, no significant improvement in hardness (ANOVA, $p>0.05$) observed upon using mannitol sprayed at 170°C (98.53 ± 15.24 N). Overall, increasing the inlet temperature resulted in a significant decline (ANOVA, $p<0.001$) in hardness of all tablets. Consequently, the harder tablets made at 110°C and 150°C exhibited significantly longer (ANOVA, $p<0.001$) disintegration times (75.33 ± 2.52 and 49.33 ± 4.51 sec) than weaker tablets made at 170°C (31.66 ± 1.53 sec). Indeed, spray dried mannitol based tablets showed 50 - 77% decrease in disintegration time from 135 ± 5.29 sec for pure mannitol to 75.33 ± 2.52, 49.33 ± 4.51 and 31.67 ± 1.53 sec for mannitol 110, 150 and 170°C respectively.

To understand the differences in mechanical properties, spray dried mannitol was characterized using Heckel profile during tableting (at-pressure) and stress/strain profile for compressed tablets at different compression forces (Table 2).

Table 2: Physico-mechanical properties of pure and spray dried mannitol made at 110 - 170°C. A and Py are intercept and yield pressure from Heckel plot respectively. AUC (area under curve, unit is Mega Joule/m^3) enclosed between loading and unloading stress/strain curves. AUC obtained from tablets compressed at 12 - 30 kN. Results reported as mean ± SD (n=3).

Mannitol	Hardness (N)	Disinte-gration Time (Sec)	Heckel Profile			Stress/Strain Elasticity Profile – AUC Between Loading/Unloading (MJ/m^3)			
			A (Inter-cept)	Py (MPa)	R^2	At 12 kN	At 14 kN	At 20 kN	At 30 kN
Pure	104.17 ± 1.70	135 ± 5.29	1.07 ± 0.02	121.59 ± 5.68	0.999	0.17 ± 0.030	0.04 ± 0.017	0.01 ± 0.004	0.01 ± 0.005
Sprayed at 110°C	258.67 ± 28.89	75.33 ± 2.52	0.87 ± 0.01	233.48 ± 13.52	0.981	0.31 ± 0.024	0.36 ± 0.024	0.42 ± 0.012	0.46 ± 0.017
Sprayed at 150°C	152.70 ± 10.58	49.33 ± 4.51	0.02 ± 0.01	32.30 ± 0.38	0.998	0.21 ± 0.030	0.30 ± 0.035	0.33 ± 0.063	0.48 ± 0.066
Sprayed at 170°C	98.53 ± 15.24	31.67 ± 1.53	0.16 ± 0.06	34.67 ± 2.65	0.999	0.20 ± 0.009	0.25 ± 0.026	0.39 ± 0.019	0.44 ± 0.014

Heckel plot's (Figure 2) terminal linear region was used to obtain the apparent yield pressure (Py) and intercept (A) as indicators of powder densification mechanism [24 - 25]. The results (Table 2) showed low Py of 32.30 ± 0.38 and 34.67 ± 2.65 MPa for mannitol spray dried at 150 and 170°C respectively which indicate plastic deformation. In contrast, pure mannitol and the one sprayed at 110°C showed significantly (ANOVA/Tukey, $p<0.001$) higher Py of 121.59 ± 5.68 and 233.48 ± 13.52 MPa respectively, indicating brittle fracture. Py value for pure mannitol was close to values reported in literature for mannitol [26]. Intercept values were significantly lower (ANOVA/Tukey, $p<0.001$) for mannitol 150 and 170°C (0.02 ± 0.01 and 0.16 ± 0.06, respectively) than for pure mannitol and mannitol 110°C (1.07 ± 0.02 and 0.87 ± 0.01, respectively). This was a further confirmation that the higher inlet temperatures resulted in more plastic behaviour and lower fragmentation. The high plasticity of mannitol produced at 150 and 170°C explained the high and moderate hardness observed for these materials.

For mannitol made at the lowest temperature 110°C, the fragmentation resulted in stronger tablets possibly due to the formation of new clean surfaces for bonding between particles under compression [27]. An example of this behaviour was also reported for other excipients, particularly lactose which fragments then yields strong tablets with Py of 178 MPa as reported by Roberts and Row [26].

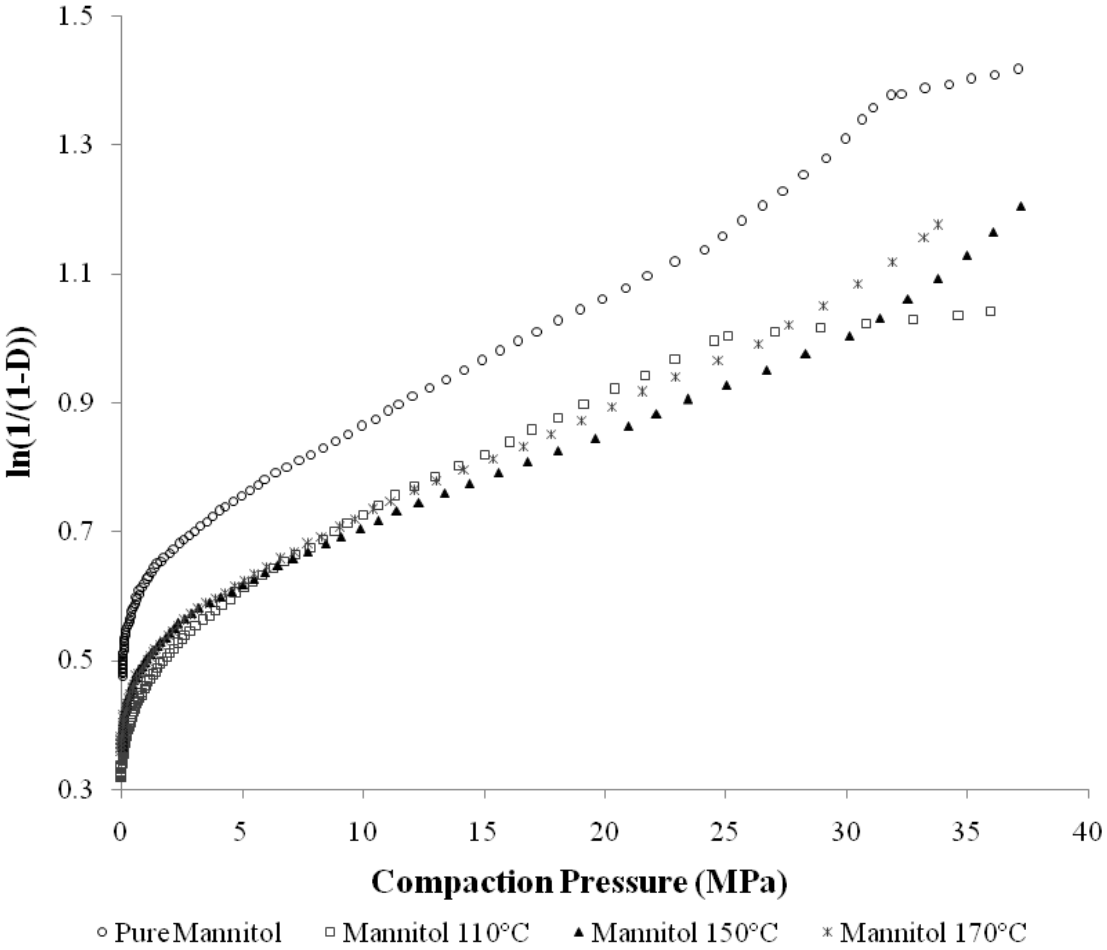

Figure 2: Heckel profile of pure and fabricated mannitol particles. Py (yield pressure) and A (intercept indicating rearrangement or fragmentation) obtained from the terminal linear region. R^2 varied between 0.981 – 0.999. Each line is representative of triplicate measurements (n=3).

SEM of mannitol compacts made at 20 kN showed significant loss of particle morphology in the order of 110°C > 150°C > 170°C. Mannitol spherical particles were more evident with the increase of inlet temperature as shown in the SEM images of tablet cross sections (Figure 1 d, f and h, observe the increase in number of arrows). At 110°C, spherical particle morphology was lost due to fragmentation mentioned earlier whereas for 150°C ductile elongation (i.e. plasticity) could be seen especially at the top and bottom of SEM image (Figure 1 f). On the other hand, particles fabricated at 170°C seemed to retain spherical morphology (Figure 1 h). This particle shape recovery of mannitol made at 170°C indicates axial elastic

recovery which is the most plausible explanation for the lower hardness and faster disintegration observed in Table 2.

Further confirmation of elastic recovery was derived from the stress/strain curves of each of the compacted specimens. Figure 3 shows each material as a compact being strained under pressure (loading) until 5% deformation is achieved before load reversal (unloading) takes place where the material undergoes elastic recovery. The initial unloading stage was accompanied with high stress released upon tablet straining before gradual strain release to original probe position. The area under curve (AUC) values between loading and unloading compressive stress/strain cycles at different compression forces are presented in Table 2 and shown in Figure 3 (highlighted area). This area represents the difference between mechanical (strain) energy per unit volume (MJ/m^3) absorbed/consumed by the material during loading and released during unloading cycles. In the case of mannitol 110 - 170°C, the energy released was higher than the energy consumed which indicates the material exhibited significant elastic recovery (Figure 3). The dissipated elastic energy (AUC) increased with the increase in compression force used to make the tablets (Table 2). This is a further confirmation of elastic recovery which was consistent with tablet capping observed at higher compression forces (up to 30 kN). In contrast, pure mannitol showed exactly the opposite effect as the mechanical energy difference (AUC) decreased with increase in compression force due to low elastic recovery tendency.

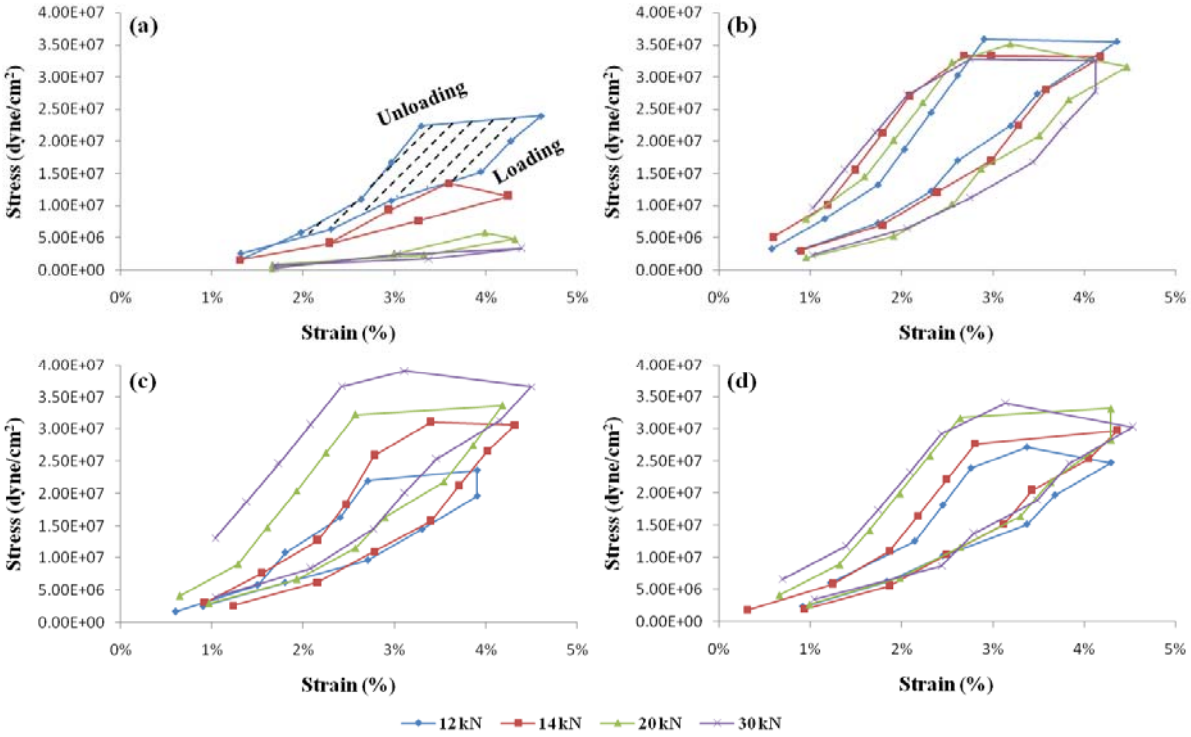

Figure 3: Compressive stress/strain loading and unloading curves, (a) pure mannitol tablet, (b) tablet of mannitol made at 110°C, (c) tablet of mannitol made at 150°C, (d) tablet of mannitol made at 170°C. Deformation target was 5% and probe speed 3 mm/sec. Specimens were compressed at 12, 14, 20 and 30 kN before testing. (a) also shows the area under curve (AUC) - highlighted - between loading and unloading which represents elastic strain energy (MJ/m^3). Each loading/unloading profile is representative of triplicate measurements (n=3).

Between the different mannitol batches, the ones sprayed at 150 and 170°C showed no significant difference in strain energy (ANOVA, $p>0.05$) between each other. Mannitol made at 110°C showed a significantly higher (ANOVA/Tukey, $p<0.05$) energy released at the low compression force of 12 kN (0.31 ± 0.024 MJ/m^3) than mannitol made at 150 (0.21 ± 0.030 MJ/m^3) and 170°C (0.20 ± 0.009 MJ/m^3), while there was no significant difference (ANOVA, $p>0.05$) at the highest compression force of 30 kN (0.46 ± 0.017, 0.48 ± 0.066 and 0.44 ± 0.014 MJ/m^3 respectively). This indicated that at the lower compression force (12 kN), mannitol 110°C exhibited higher elastic recovery capacity than mannitol 150 and 170°C that was hampered due to fragmentation at the higher compression force (30 kN).

For all three mannitol formulations, the spherical particles behaved like 'micro-sponges' that resisted fracture especially in the case of mannitol 150 and 170°C where the air entrapped in the pores resisted compressive stress in the axial direction [28]. According to [29], strains are magnified about regions of low density and upon releasing the force, a mechanical failure may occur which leads to capping. Moreover, the formation of a continuous crust on the particle surface during spray drying (which will be discussed under particle formation mechanisms), also proved to be resistant to crushing, hence the particles in Figure 1 (especially h) retained their original shape.

Particle formation mechanisms

The influence of spray drying temperature on particle formation and pore generation was studied using hot stage microscopy. Drying of liquid droplets of the optimum formulation mixture (mannitol 10% w/v and ammonium bicarbonate 5% w/v) at different temperatures (110-170°C) revealed different crystallization kinetics. All the formulations showed bursting gas bubbles indicating NH_4HCO_3 decomposition into $H_2O\uparrow$, $CO_2\uparrow$ and $NH_3\uparrow$ during mannitol particle formation. At the lowest temperature 110°C, crystallization of mannitol occurred almost instantly (Figure 4 a and b) due to the strong tendency of mannitol to crystallize [30].

The formulation dried at 150°C showed different drying kinetics to that of the formulation at 110°C. The droplet formed a smooth continuous crust at the surface with small patches of pores (appear as black dots in Figure 4 c and d). Upon puncturing the droplet using a thin needle, the surface layer was removed easily revealing mannitol crystals slowly growing inside the particle (Figure 4 e and f). This interesting drying behaviour was attributed to slower crystallization of mannitol particles at this temperature which resulted in better organization of the crystals on the surface of droplet and hence regular shaped spherical particles were formed (SEM in Figure 1 e).

At 170°C, hot stage images were unobtainable due to inability of mannitol to crystallize above its melting point of 165°C resulting in dark images with no features. However, in reality spray drying temperature

vary along the chamber and through the cyclone down to the collector. The outlet temperature is always lower than the inlet temperature and resulted in crystallization of mannitol between 90 and 100°C.

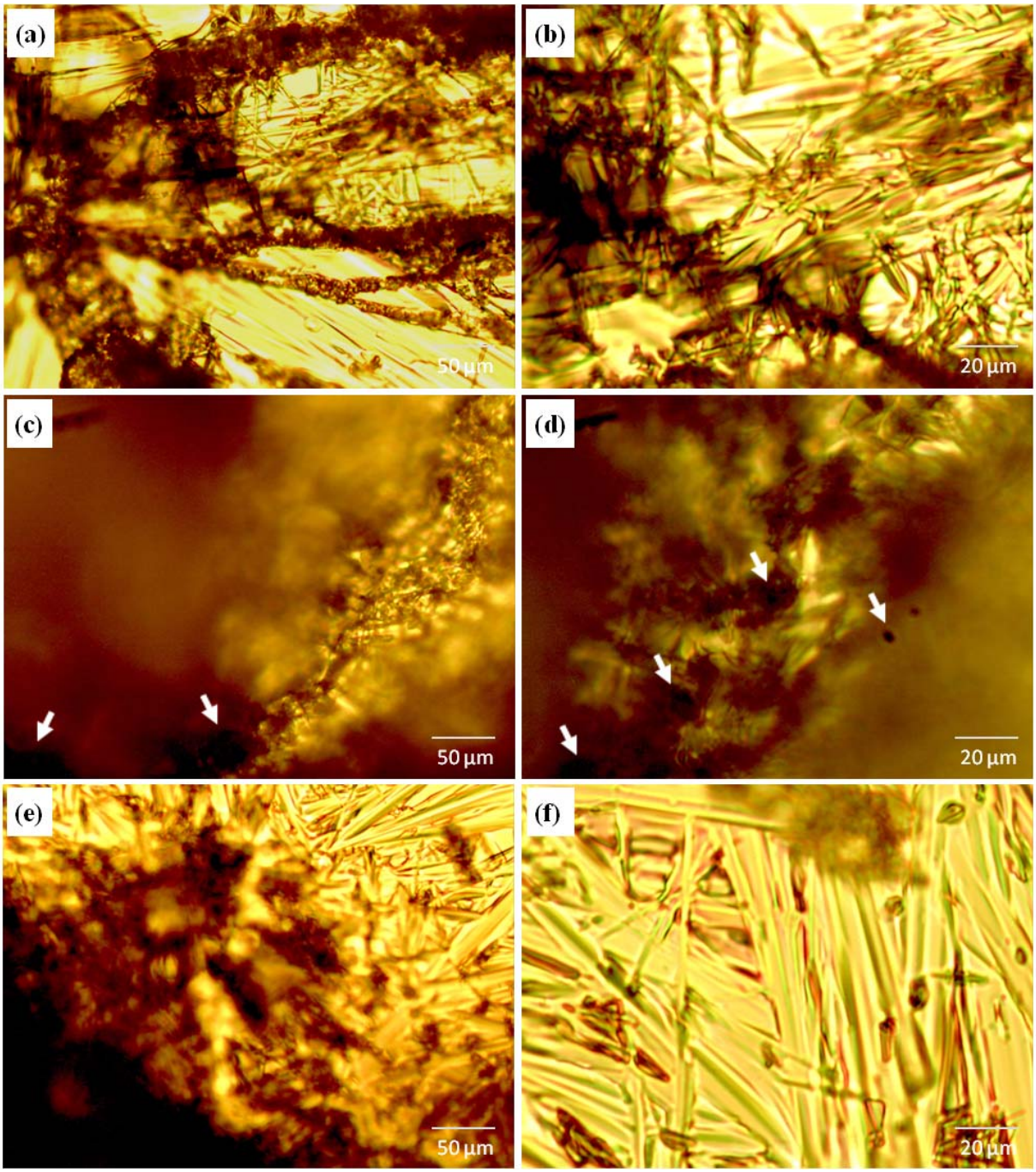

Figure 4: HSM images of mannitol (10% w/v) and NH_4HCO_3 (5% w/v) droplets dried on a preheated hot stage microscope slide at 110°C (a and b), 150°C (c and d), 150°C (e and f) after removal of surface crust using a thin needle to reveal growing crystals. Arrows show surface pores formed during the process.

Thermal and polymorphic properties

Thermal and polymorphic profiling methods (DSC, TGA and XRD) were utilized to understand spray dried mannitol particular physico-mechanical properties. DSC scans showed a 3°C shift (ANOVA, $p<0.001$) in melting onset from 165.51 ± 0.13°C for pure mannitol to 162.18 ± 0.43 - 162.86 ± 0.11°C for mannitol 110-170°C respectively (Figure 5). TGA also confirmed a slight difference between pure and spray dried mannitol (Figure 5) as the latter showed a step transition pertinent to weight loss at 166.88°C which was absent from pure mannitol. There was a trend for weight loss at this temperature which followed the order from the highest: 110°C (0.81 ± 0.07%) > 150°C (0.51 ± 0.12%) > 170°C (0.43 ± 0.15%). This in turn confirms the loss was dependant on spray drying temperature and could be explained by volatilization of some entrapped water subsequent to melting of mannitol at 162°C. A further confirmation of this event is the moisture content of produced powders which was slightly higher than pure mannitol (Table 1). TGA was also used to confirm the decomposition temperature of pure ammonium bicarbonate that was confirmed to occur at 60°C (Figure 5).

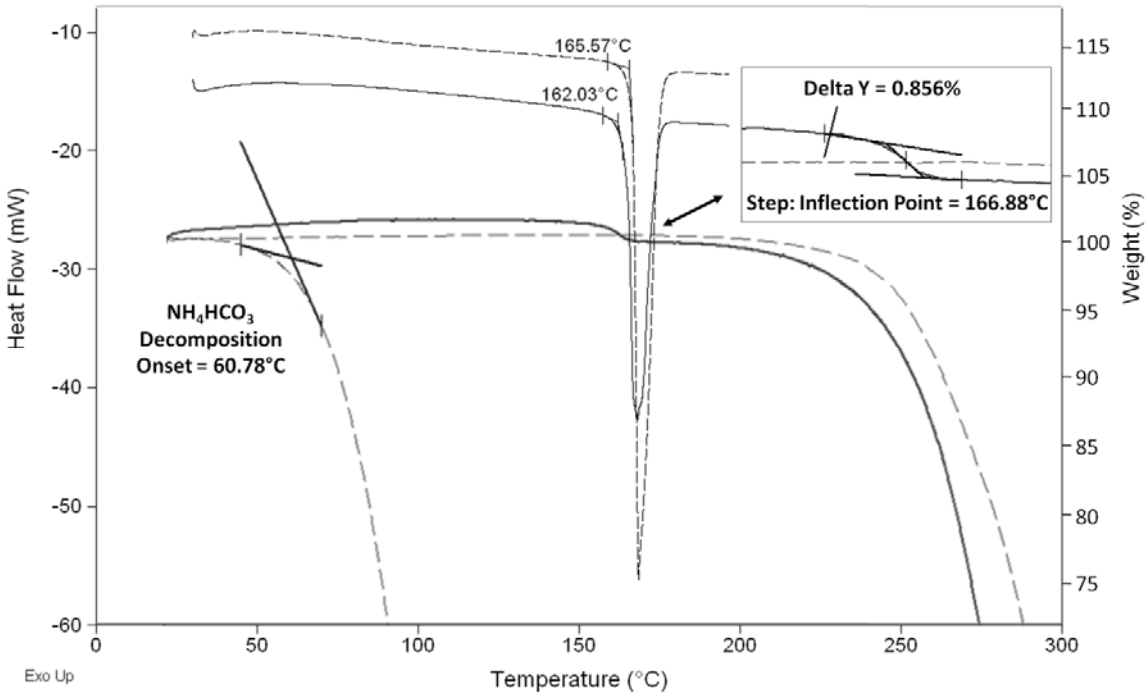

Figure 5: Overlaid DSC and TGA representative thermograms of pure mannitol (dashed lines), spray dried mannitol (solid lines) and ammonium bicarbonate (dashed on the left). DSC and TGA thermograms are representative of triplicate measurements (n=3).

DSC also showed a significant increase (ANOVA/Tukey, $p<0.05$) of melting onset upon increase in the spray drying inlet temperature between 110 and 170°C. The small differences in melting onsets (162.18 ± 0.43 to 162.86 ± 0.11°C) were attributed to generation of different polymorphs of mannitol [16]. No significant difference (ANOVA, $p>0.05$) in enthalpy of fusion was found between the spray dried (243.33 ± 3.84 – 245.53 ± 8.57 J/g for 110 - 170°C) and pure mannitol (246.83 ± 1.40 J/g) powders. This meant that even if different polymorphs existed, they are very closely related as the energy required to melt the materials was almost similar. In fact, similar observation was reported by Burger et al. [16] for the small energetic differences of D-mannitol β and α polymorphs which were manifested with small differences in heats of fusion.

Using XRD, no amorphous phase was detectable and it was not in the interest to seek more sensitive techniques because mannitol is known to be a poor glass former [30]. However, XRD confirmed the presence of polymorphic forms as anticipated. Figure 6 shows that pure mannitol is crystalline made up of 99.98% w/w β type whereas mannitol spray dried at 110 - 170°C is also crystalline made up of mixtures of β and α polymorphs. No δ polymorph (thermodynamically unstable form) could be observed which is consistent with the DSC results (no melting peak at 155°C).

The observed polymorphic forms have different compression profiles under pressure as reported earlier by Burger et al. [16], which ultimately contributed to the particular plasticity or fragmentation behaviours. Interestingly, the use of ammonium bicarbonate during spray drying of mannitol led to the appearance of α polymorph in contrast to observations by Hulse et al. [17] which reported conversion of commercial mannitol (sprayed alone) to β type upon re-spray drying. Despite this, our results agree with Maas et al. [18] who reported that α polymorph exists alongside β polymorph and that its amount increases with the increase of spray drying outlet temperature. The fraction of α polymorph increased from 3.23 to 84.1% w/w upon increasing the inlet temperature from 110-170°C. Concomitantly, the fraction of β polymorph decreased from 96.77 to 15.89% w/w under the same conditions.

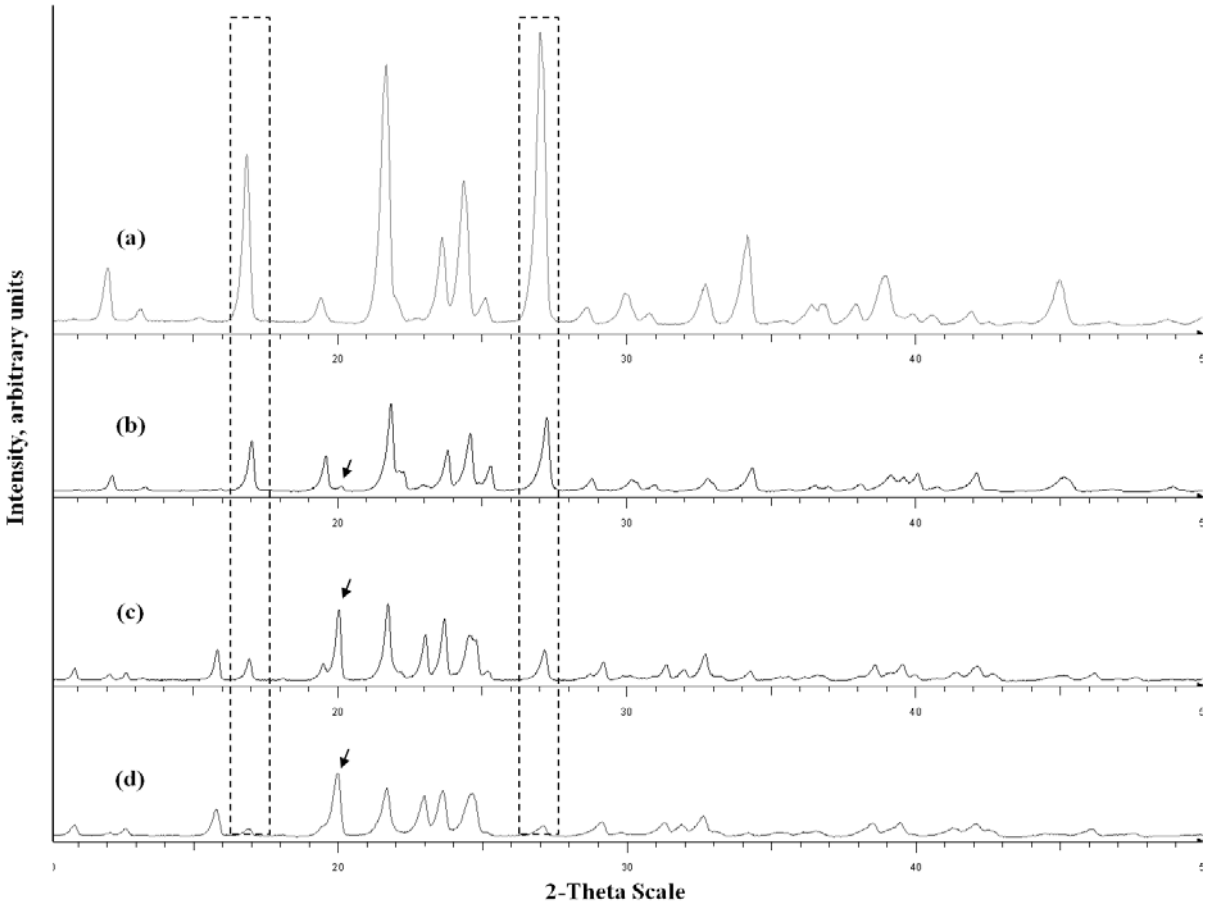

Figure 6: XRD for pure and spray dried mannitol powders. (a) pure mannitol, (b) mannitol made at 110°C, (c) mannitol made at 150°C and (d) mannitol made at 170°C. The dashed rectangles show a declining intensity for β polymorph at 2θ 16° and 26°. The arrows show an increased intensity of α polymorph peak at 2θ 20°. Each XRD pattern is representative of triplicate scans (n=3).

As a result, mannitol made at 110°C showed brittle fracture (fragmentation) profile as the mixture has a significant amount of β polymorph (96.77% w/w). However, the high hardness observed could be attributed to the presence of 3.23% w/w α polymorph (appearing at 2θ of 20°) that act, due to lower die friction and better compressibility [16], as a binder between the clean surfaces resulting from fragmentation of β polymorph. On the other hand, mannitol made at 150 and 170°C showed high hardness related to the increase in α polymorph (63.2 and 84.1% w/w respectively) which is the predominant polymorph at these temperatures.

XRD carried out on tablets showed no difference between patterns obtained for powders and after tableting which confirms no crystallographic changes have occurred during compression. Moreover, the elastic recovery tendency of spray dried mannitol tablets observed earlier could also be related to the mixture of polymorphic forms constituting the powders. The resultant mixture of polymorphs leads to non-homogeneity and anisotropy of the tablet base [31 - 33]. Therefore, the tablets exhibited capping tendency at high compression forces despite the radial strength (diametral crushing strength) being quite high.

Conclusion

Spray drying mannitol resulted in higher porosity due to evaporation of ammonium bicarbonate and increased hardness due to changing particle densification mechanism. The resultant particles retained surface pores produced due to ammonium bicarbonate decomposition and gas expulsion through the forming crust. The porosity significantly increased for both powder and tablets in comparison with pure mannitol and was responsible for the faster disintegration of ODTs due to wicking action.

Spray drying temperature significantly affected the particles' micromeritic, physico-mechanical and polymorphic properties. Tablets made from engineered mannitol showed a significant increase (up to 150%) in hardness and reduction (50 - 77%) of disintegration time in comparison with pure mannitol. Mannitol particles made at low temperature showed densification by fragmentation followed by particle bonding. Fragmentation possibly occurred due to strong tendency of mannitol to crystallize at the low temperature resulting in irregular crystalline particle morphology. The produced particles were more susceptible to fracture under pressure. In addition, the polymorphic composition of the powder at low temperature revealed it had a significant proportion of β polymorph (besides α polymorph) which is well known to undergo brittle fracture.

On the other hand, mannitol particles made at the higher inlet temperatures showed more flexibility under compression (plasticity) due to the formation of a smooth crust on the droplet surface during spray drying.

The smooth crust formation was attributed to slower crystallization of mannitol particles at the higher temperatures which resulted in better organization of the crystals on the surface of droplet and hence regular shaped spherical particles were formed. The high hardness resulted from mannitol particles at high temperatures was also related to further increase in α polymorph which is the predominant polymorph at these temperatures and is known to exhibit lower die friction and better compressibility. However, the flexibility and relatively high internal porosity, especially at 170°C, resulted in the particles retaining high elastic strain energy. The latter was responsible for elastic recovery tendency observed for the spray dried mannitol particles.

Acknowledgments

The authors would like to thank Aston University for providing Ali Al-Khattawi with Overseas Bursary Scholarship towards his PhD. They are also grateful for financial support from Colorcon Ltd and ARCHY for co-funding Jasdip Koner's studentship. The authors would also like to thank Dr Stephen Barton and Dr Simon Demas from Kingston University for their help with hot stage microscopy.

References

[1] C. Telang, R. Suryanarayanan, and L. Yu, Crystallization of D-mannitol in binary mixtures with NaCl: phase diagram and polymorphism., Pharm. Res. 20 (2003) 1939–1945.

[2] A. Al-khattawi and A. R. Mohammed, Compressed orally disintegrating tablets: excipients evolution and formulation strategies., Expert Opin. Drug Deliv. 10 (2013) 651–663.

[3] H. L. Ohrem, E. Schornick, A. Kalivoda, and R. Ognibene, Why is mannitol becoming more and more popular as a pharmaceutical excipient in solid dosage forms?, Pharm. Dev. Technol. 19 (2014) 257–262.

[4] N. C. Alderborn G, Pharmaceutical powder compaction technology, 1st ed. New York: Marcel Dekker, 1996.

[5] T. Yoshinari, R. T. Forbes, P. York, and Y. Kawashima, The improved compaction properties of mannitol after a moisture-induced polymorphic transition., Int. J. Pharm. 258 (2003) 121–131.

[6] Y. Fu, S. Yang, S. H. Jeong, S. Kimura, and K. Park, Orally Fast Disintegrating Tablets: Developments, Technologies, Taste-Masking and Clinical Studies, Crit. Rev. Ther. Drug Carrier Syst. 21 (2004) 433–476.

[7] R. Vehring, Pharmaceutical particle engineering via spray drying., Pharm. Res. 25 (2008) 999–1022.

[8] C. Gervelas, A.-L. Serandour, S. Geiger, G. Grillon, P. Fritsch, C. Taulelle, B. Le Gall, H. Benech, J.-R. Deverre, E. Fattal, and N. Tsapis, Direct lung delivery of a dry powder formulation of DTPA with improved aerosolization properties: effect on lung and systemic decorporation of plutonium., J. Control. Release. 118 (2007) 78–86.

[9] D. M. El-Sherif and M. A. Wheatley, Development of a novel method for synthesis of a polymeric ultrasound contrast agent., J. Biomed. Mater. Res. A. 66 (2003) 347–355.

[10] K. Koizumi, Y. Watanabe, K. Morita, N. Utoguchi, and M. Matsumoto, New method of preparing high-porosity rapidly saliva soluble compressed tablets using mannitol with camphor, a subliming material, Int. J. Pharm. 152 (1997) 127–131.

[11] K. Masters, Spray drying handbook., Ed. 3, 1979.

[12] Y. Gonnissen, J. P. Remon, and C. Vervaet, Development of directly compressible powders via co-spray drying., Eur. J. Pharm. Biopharm. 67 (2007) 220–226.

[13] J. Rojas and V. Kumar, Effect of polymorphic form on the functional properties of cellulose: A comparative study, Carbohydr. Polym. 87 (2012) 2223–2230.

[14] H. S. Kim, G. A. Jeffrey, and R. D. Rosenstein, The crystal structure of the K form of D-mannitol, Acta Crystallogr. Sect. B Struct. Crystallogr. Cryst. Chem. 24 (1968) 1449–1455.

[15] H. M. Berman, G. A. Jeffrey, and R. D. Rosenstein, The crystal structures of the α' and β forms of D-mannitol, Acta Crystallogr. Sect. B Struct. Crystallogr. Cryst. Chem. 24 (1968) 442–449.

[16] A. Burger, J. O. Henck, S. Hetz, J. M. Rollinger, A. A. Weissnicht, and H. Stöttner, Energy/temperature diagram and compression behavior of the polymorphs of D-mannitol., J. Pharm. Sci. 89 (2000) 457–468.

[17] W. L. Hulse, R. T. Forbes, M. C. Bonner, and M. Getrost, The characterization and comparison of spray-dried mannitol samples., Drug Dev. Ind. Pharm. 35 (2009) 712–718.

[18] S. G. Maas, G. Schaldach, E. M. Littringer, A. Mescher, U. J. Griesser, D. E. Braun, P. E. Walzel, and N. A. Urbanetz, The impact of spray drying outlet temperature on the particle morphology of mannitol, Powder Technol. 213 (2011) 27–35.

[19] USP Convention, Bulk Density and Tapped Density of Powders <616>. Maryland: United States Pharmacopeia, 2012.

[20] A. Al-Khattawi, H. Alyami, B. Townsend, X. Ma, and A. R. Mohammed, Evidence-based nanoscopic and molecular framework for excipient functionality in compressed orally disintegrating tablets., PLoS One. 9 (2014) e101369.

[21] USP Convention, Disintegration <701>. Maryland: United States Pharmacopeia, 2005.

[22] G. Reineccius and W. Bangs, Spray drying of food flavors. III. Optimum infeed concentrations for the retention of artificial flavours, Perfum. flavorist. 10 (1985) 27–29.

[23] M. Re, Microencapsulation by Spray Drying, Dry. Technol., 16, pp. 1195–1236, 1998.

[24] R. W. Heckel, Density-Pressure Relationships in Powder Compaction, Trans. Metall. Soc. AIME. 221 (1961) 671–675.

[25] J. A. Hersey and J. E. Rees, Deformation of Particles During Briquetting, Nat. Phys. Sci. 230 (1971) 96.

[26] R. J. Roberts and R. C. Rowe, The compaction of pharmaceutical and other model materials - a pragmatic approach, Chem. Eng. Sci. 42 (1987) 903–911.

[27] M. Jivraj, L. G. Martini, and C. M. Thomson, An overview of the different excipients useful for the direct compression of tablets, Pharm. Sci. Technolo. Today. 3 (2000) 58–63.

[28] O. Antikainen and J. Yliruusi, Determining the compression behaviour of pharmaceutical powders from the force–distance compression profile, Int. J. Pharm. 252 (2003) 253–261.

[29] P. J. Jarosz and E. L. Parrott, Factors influencing axial and radial tensile strengths of tablets, J. Pharm. Sci. 71 (1982) 607–614.

[30] L. Yu, D. S. Mishra, and D. R. Rigsbee, Determination of the glass properties of D-mannitol using sorbitol as an impurity., J. Pharm. Sci. 87 (1998) 774–777.

[31] D. Train, Transmission forces through a powder mass during the process of pelleting, Trans. Inst. Chem. Eng. 35 (1957) 258–266.

[32] A. Kandeil, M. C. de Malherbe, S. Critchley, and M. Dokainish, The use of hardness in the study of compaction behaviour and die loading, Powder Technol. 17 (1977) 253–257.

[33] C. Nyström, K. Malmqvist, J. Mazur, W. Alex, and A. W. Hölzer, Measurement of axial and radial tensile strength of tablets and their relation to capping., Acta Pharm. Suec. 15 (1978) 226–232.